

Tribology of laser modified surface of stainless steel in physiological solution

RAGHUVIR SINGH

Department of Materials Science and Engineering, The University of Tennessee, Knoxville, TN 37996, USA

NARENDRA B. DAHOTRE*

Department of Materials Science and Engineering, The University of Tennessee, Knoxville, TN 37996, USA; Materials Processing Group, Metals and Ceramics Division, Oak Ridge National Laboratory, Oak Ridge, TN 37831, USA

Published online: 25 August 2005

The laser surface treatment of stainless steel (SS) 316L, an important alloy for biomedical applications, was used to improve its corrosion and wear-corrosion resistance in bio-environment. Microstructural and X-ray diffraction (XRD) pattern analysis showed presence of an austenitic phase in both untreated and laser-treated SS316L. Laser melting produced homogenized and refined microstructure on the surface with higher hardness (143–171 HV) compared to untreated SS316L (131 HV). Increase in intensity of γ (200) peaks in XRD pattern for laser-treated (>800 W) SS316L indicated possible crystallographic orientation along γ (200) plane. Passive currents were reduced to $<2.8 \mu\text{A}/\text{cm}^2$ and pitting potentials was increased to $>+344$ mV for samples laser surface treated at greater than 1200 W. The volume-loss and wear-rate of laser-treated SS316L were significantly reduced compared to untreated sample. Abrasive wear was the main wear mechanism for both untreated and laser surface treated SS316L. Wear particles/debris were found to be cold welded on the surface of SS316L and showed brittle cracking with further wear-straining.

© 2005 Springer Science + Business Media, Inc.

1. Introduction

The application of stainless steels in surgical fields has begun in 1926 and since then it has been increasingly used in orthopaedic surgery for internal fixation devices such as plates, nails, etc. [1–6]. It possesses a combination of good mechanical strength, ductility, corrosion resistance, and fabrication properties and available at relatively low cost. Lately, increasing metal-ion related complexities (especially due to Ni, Be, Co, Cr, Ta, Ti and V ions) after long-term exposure questioned the reliability of biomaterials. The metal ions and wear debris from corrosion and wear reaction have been frequently reported in the surrounding tissues that affected the cell morphology, growth, and its functioning [7, 8]. Yet, large usage of stainless steel (316L) for orthopaedic devices is primarily due to its lower cost by 1/10th to 1/5th of Co-Cr alloys, commercially pure Ti, and titanium alloys [9]. The demands for long-term usage of implant devices and minimal toxic effects due to metal ions to get rid of painful surgery have stressed to improve or develop better materials for orthopaedic application [10–15]. While improving and developing materials for bio-medical application, corrosion and wear properties

(being root cause of deterioration) have been on the forefront of the field of research.

Surface modification has been widely employed as an economical alternative for improving corrosion and wear resistance and bioactivity of existing materials (such as stainless steel, Ti-alloys, and Co-Cr alloys). It has an additional advantage as it preserves the useful properties of bulk material and can offer a biocompatible surface desirable for bio-environment. Among various methods of surface modification, laser induced surface modification has emerged as an increasingly desirable technique due to several special features associated with it. Laser surface modification derives its attractiveness in engineering applications mainly due to (i) formation of a small heat-affected zone (ii) refinement and homogenization of microstructure leading to enhanced mechanical properties and corrosion resistance, (iii) the possibility of forming novel surface alloys unattainable by other methods because of non-equilibrium nature of the process. Relatively rapid rate of processing, ease of automation, operation at atmospheric pressure, and selective area treatment are additional advantages over other surface modification

*Author to whom all correspondence should be addressed.

techniques. The CO₂, Nd-YAG, and excimer lasers have been commonly used to improve the pitting, cavitation, and intergranular corrosion resistance of stainless steel [16–30]. Laser is relatively less commonly used for surface modification of biomedical materials. Several studies indicated that the laser surface melting significantly increased the pitting potential of stainless steels [21–30]. However, its effect on the wear-corrosion resistance of stainless steels in bio-environment is yet to be unveiled.

An attempt has been made to investigate the effects of laser surface melting on the microstructure, corrosion resistance, and wear-corrosion of stainless steel in Ringer's solution. This was accomplished by surface melting using a 2.5 kW Hobart continuous wave Nd:YAG laser at power ranging from 800–1500 W. The specimens were subsequently studied for corrosion and wear-corrosion resistance using electrochemical polarization and pin-on-disc sliding methods respectively. The corrosion resistance was evaluated in terms of passivation current and pitting potential and wear resistance was expressed in volume-loss (mm³) and wear-rate (mm³/m).

2. Materials and methods

Stainless steel AISI 316L (%wt: C-0.03, Mn-2.0, P-0.045, Si-0.75, Cr-18, Ni-9.7%, Mo-2.0, Fe-balance) was selected for this study, as it is an important biomedical alloy.

A 2.5 KW Hobart continuous wave Nd:YAG laser equipped with a fiber optics beam delivery system was employed for laser surface melting (LSM) operation. Parallel tracks with partial overlapping (~15%) were

laid with the laser beam focused 0.5 mm above the surface of the substrate to get a beam spot size of ~3.8 mm on surface of the sample. A laser beam with power ranging from 800–1500 W was used over a set of samples keeping the laser traverse speed and working distance constant. The laser surface melting was carried out with argon as cover gas. The laser treatment parameters are listed in Table I.

For electrochemical studies, coupons of 20 × 20 × 3 mm³, were cut from the laser-treated plates using TechCut10 high-speed abrasive wheel (Allied High Tech Products Inc). The polishing to reveal microstructure of untreated and laser surface treated SS316L was performed firstly by grinding them on a series of grit papers ranging from 240–1200 grit followed by cloth polishing with 0.03 μm size alumina slurry. All specimens were cleaned to degrease in acetone before they were immersed in the experimental solution for electrochemical polarization. The etching to reveal the microstructure of untreated and laser-treated SS316L was done in the solution of 10 ml HNO₃ + 15 ml HCl + 10 ml acetic acid at ambient temperature.

The microstructural characterization and morphology of worn surface were revealed using optical microscope (Nickon, Epiphot, Japan) and Hitachi 3500 Variable Pressure scanning electron microscope (SEM) respectively. Evolution of phases and possible changes in crystallographic orientations due to laser surface melting were identified by the Philips Norelco X-ray diffractometer with Cu Kα (1.54 Å wavelength) radiation operated at 20 kV and 10 mA. Hardness of untreated and laser-treated SS316L was determined under 100 g normal load applied for 15 s using Micromet 2100 Series Microhardness tester (Buehler).

The electrochemical polarization studies were conducted in non-deaerated Ringer's physiological solution. The solution was prepared by adding 9 g/l NaCl, 0.17 g/l CaCl₂, 0.04 g/l KCl, and 2.0 g/l NaHCO₃ (A. R. grade chemicals) to distilled water. Anodic polarization experiments were conducted at 37°C to simulate the body temperature. Specimens for these tests were mounted in the epoxy and ensured no crevice

TABLE I Laser processing parameters

Sample	Laser power (Watt)	Laser speed (mm/min)
LSM 800	800	1000
LSM 1000	1000	
LSM 1200	1200	
LSM 1500	1500	

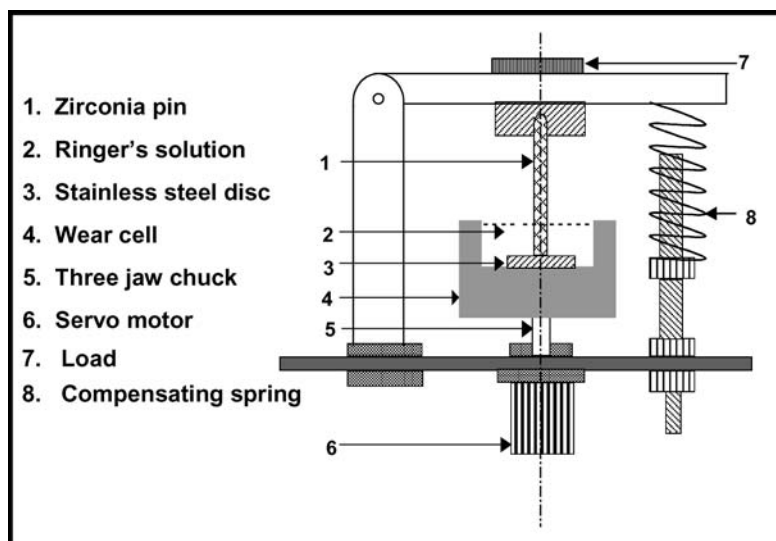


Figure 1 Pin-on-disc wear set-up.

formation occurred at the contact surface between epoxy and metal after the polarization test. The reproducibility of data was ensured by repeating the tests for three times (for anodic polarization). Specimens were cathodically cleaned at -1000 mV for 120 seconds to remove oxides, if any, on the specimen's surface before scanning was commenced. The anodic polarization experiments were initiated from -200 mV with respect to open circuit potential at a scan speed of 0.17 mV/s. Saturated calomel electrode (SCE) and graphite electrode were used as a reference and a counter electrodes respectively during electrochemical polarization experiments. All values of potential in this paper are reported with respect to SCE. Electrochemical experiments were performed using computer controlled VersaStat II, Potentiostat/Galvanostat (EG&G, Princeton Applied Research).

During wear-corrosion test, 50 mm long and 3 mm diameter zirconia pin was used as a counter surface. The zirconia pin was chosen because it is a frequently used material for ceramic cup that mates with the metallic stem or ceramic head in total hip replacement (THR) surgery. The flat base (contact surface) of zirconia pin was prepared by abrading and polishing against a series of emery papers ranging from 240–600 grit as suggested elsewhere [14]. The wear surface was fabricated from untreated and laser-treated SS316L in the size of $15 \times 15 \times 3$ mm³. The disc was held fixed by the sample stage at the bottom of a cylindrical wear cell. The wear cell was filled with Ringer's solution to the level so that the disc remained immersed in the solution. The wear cell was rotated at a preset linear speed and distance using computer-controlled motor. Zirconia pin was held fixed in contact with the disc and disc was allowed to rotate at a constant speed. The latter was rotated at a speed of 0.042 m/s for 300, 600, and 900 m to observe the effect of distance on wear under the normal load of 0.9 kg. A fresh sample was used for wear experiment conducted for each distance (300 m, 600 m, and 900 m). The schematic of wear set-up is illustrated in Fig. 1. The weight-loss in pin and SS316L disc was determined with resolution of 0.0001 g using Sartorius electronic digital balance. The volume-loss was calculated by measuring the worn surface area multiplied by average track depth. The depths of the wear tracks were measured using roughness profilometer (perthometer M1 with PFM drive unit, Mahr GMBH Germany). The stylus tip was set to travel across the wear track at 10 different locations and average of depth at these locations was an average track depth, used for volume-loss determination.

3. Result and discussions

3.1. Microstructure

The microstructures of the regions of untreated and laser surface treated SS316L in cross section are shown in Fig. 2. The untreated SS316L showed equiaxed austenitic grains (~ 43 μ m), which on laser melting and resolidification produced columnar structure in the surface region. The laser treatment resulted in refinement and homogenization of microstructure with columnar

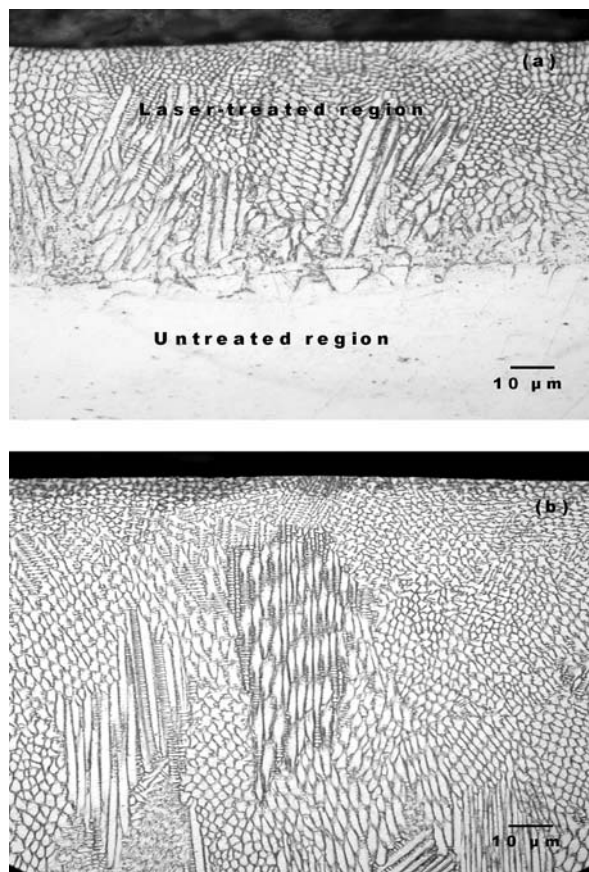


Figure 2 Microstructure of laser-treated SS 316L at (a) 800 W and (b) 1500 W power.

grain ranging from 8 – 12 μ m in the outermost surface. Fig. 2 also showed variation in dendrite size and their orientation at different laser powers. This difference could be due to increase in the molten volume with laser power consisting of larger thermal-gradient than that at the low laser powers. It has been shown earlier that the higher depth of the melt-pool indicated high molten volume [31–33]. The specimen treated at increasing laser power from (800, 1000, 1200, 1500 W) produced the depth of melt pool in order as $132 < 163 < 293 < 469$ μ m respectively which indicated increase in molten volume. Both untreated and laser-treated stainless steel contained austenitic (γ) phase as indicated by X-ray diffraction (XRD) pattern shown in Fig. 3. Increase in relative intensity of γ (200) peak with laser power from 800–1500 W is an indication of possible crystallographic orientation (Fig. 3). This is, however, under further investigation for detailed understanding of the textural developments and will be presented in future.

The micro-hardness values were higher for laser-treated than untreated stainless steel (131 HV) as listed in Table II. Hardness in laser-resolidified region varied such that the cellular regions (165–171 HV) were harder than the columnar regions (143–152 HV) for various treated stainless steels.

3.2. Electrochemical polarization behavior

The anodic polarization behavior of untreated and laser surface treated stainless steel in Ringer's

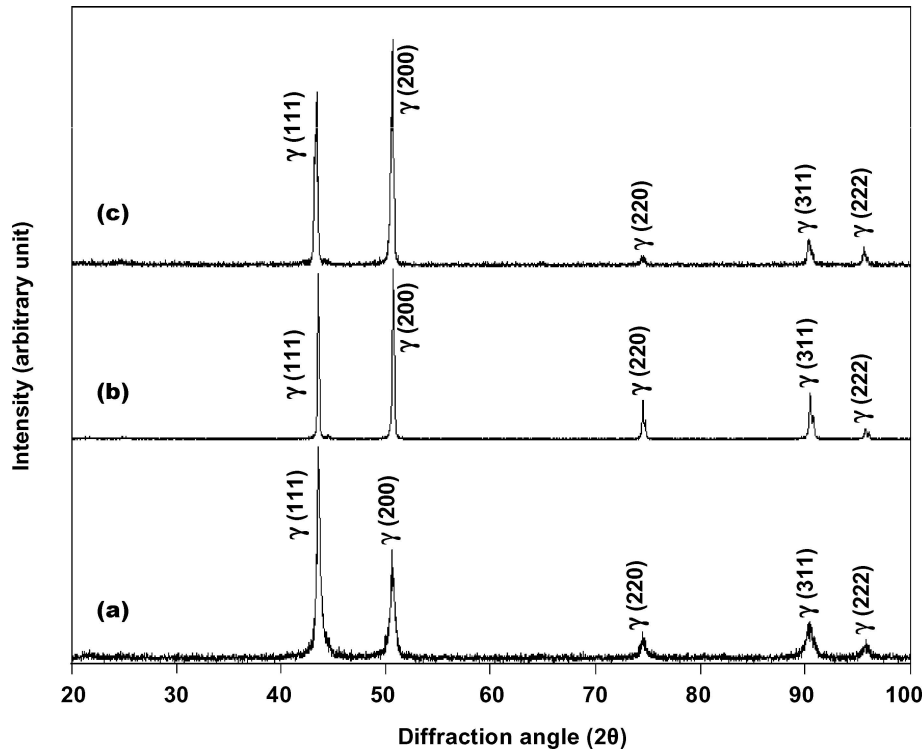


Figure 3 X-ray diffraction pattern of SS316L (a) Untreated, (b) Laser-treated at 800 W, and (c) Laser-treated at 1500 W.

physiological solution is presented in Fig. 4. The corrosion potential of laser-treated stainless steel was more noble than the untreated SS316L and listed in Table III.

TABLE II Variation in micro-hardness of laser-treated stainless steel

Laser power	Micro-hardness of cellular region (HV)	Micro-hardness of columnar region (HV)
Untreated	131 ± 11	–
800	165 ± 9	152 ± 5
1000	165 ± 12	149 ± 8
1200	171 ± 6	143 ± 8
1500	168 ± 5	143 ± 4

The untreated SS316L showed it to be -131 mV and it rose to -17 to $+49$ mV after laser surface treatment (Table III and Fig. 4). The more noble corrosion potential in active-passive alloy is an indication of formation of a stable passive surface film for lower corrosion. Passivation current densities after laser treatment were significantly reduced compared to untreated SS316L. The passivation current density for untreated SS316L was $\sim 8 \mu\text{A}/\text{cm}^2$ and was reduced to below $2.8 \mu\text{A}/\text{cm}^2$ after laser surface treatment (Fig. 4). X-ray diffraction pattern of laser-treated SS316L showed indication of possible crystallographic orientation of γ along (200) planes. The latter component became

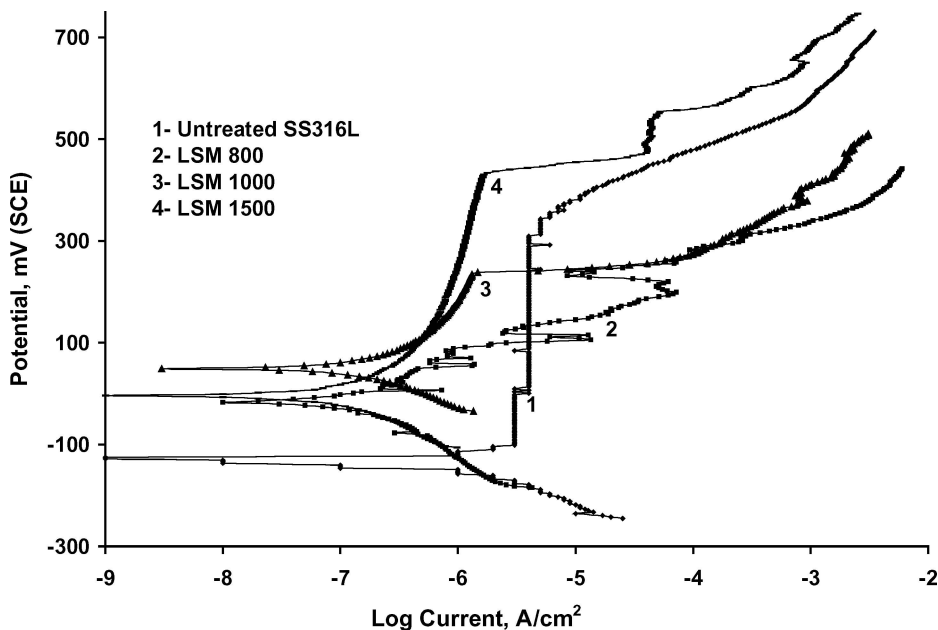


Figure 4 Anodic polarization behavior of untreated and laser-treated stainless steel in Ringer's physiological solution.

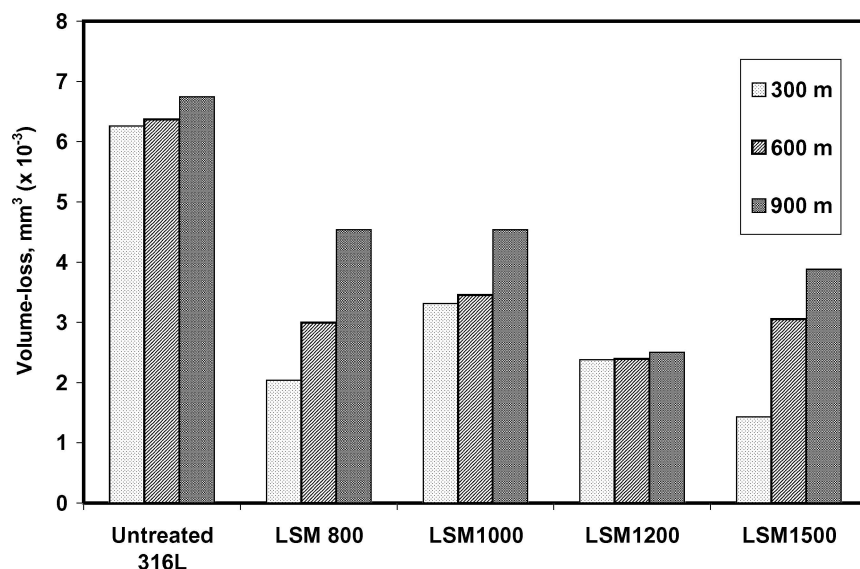


Figure 5 Volume-loss during wear-corrosion of untreated and laser-treated SS316L.

increasingly prominent with increase in laser power (>1000 W), as observed from the relative peak intensities (Fig. 3). These textural changes could be one of the attributes for improvement of passive film properties of stainless steel.

The pitting corrosion resistance of laser-processed SS316L was found to vary with laser powers (Table III). The pitting potential of laser-treated at >1200 W ($>+344$ mV) was more noble than the untreated SS316L ($+310$ mV), whereas, those laser-treated at <1200 W power showed lower pitting potential ($<+235$ mV) than untreated stainless steel ($\sim+310$ mV). Earlier studies showed pitting resistance (for super austenitic stainless steel and nickel based alloys) to vary with laser scanning velocity [34]. Some investigations showed improvement in pitting resistance after laser surface treatment of SS304 due formation δ ferrite and crystallographic orientation [25, 29]. The formation of δ ferrite reported to depend on the laser scanning parameters including cooling rate [25, 29]. On the contrary, in the present study, although XRD results (Fig. 3) of laser surface treated SS316L indicated the absence of δ ferrite, the specimen treated at >1200 W showed improvement in pitting corrosion resistance. Possible crystallographic orientation along γ (200) more than along γ (111) (at >1000 W laser power) in laser-treated stainless steel could enhance the pitting resistance of SS316L. It has also been investigated earlier that the crystallographic orientation due to cold rolling has certain influence on pitting potential

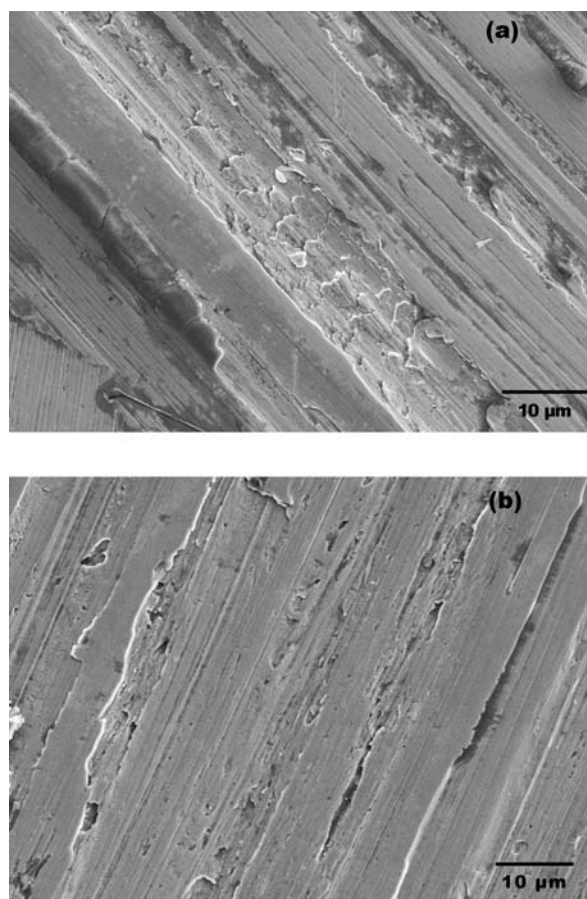


Figure 6 Morphology of wear tracks in (a) Untreated and (b) LSM 1500 SS316L.

TABLE III Electrochemical parameters of untreated and laser-treated SS316L

Laser power	Corrosion potential (E_{corr}) (mV)	Pitting potential (mV)	Passive current density ($\mu\text{A}/\text{cm}^2$)
Untreated	-131	+310	8.0
800	-17	+124	6.3
1000	-1	+235	<2.8
1200	+21	+344	<2.8
1500	+49	+431	<2.8

of stainless steels 304 [35–37]. In addition to this, homogenization of microstructure also contributes to improvement in the corrosion properties. The manganese sulfide (MnS) and TiN inclusions are considered to be active sites for pit initiation in stainless steels and nickel-based alloys in chloride containing solution [25, 29, 38]. Such sites in steels are likely to be eliminated by homogenization during laser surface melting and so enhancement in the pitting corrosion resistance may be achieved.



Figure 7 Brittle cracking on the wear track of untreated SS316L.

3.3. Wear-corrosion

The volume-loss due to wear-corrosion is shown in Fig. 5. The figure clearly indicates lower volume-loss from laser-treated specimens ($1.43 \times 10^{-3} \text{ mm}^3$ to $4.54 \times 10^{-3} \text{ mm}^3$) compared to untreated ($6.26 \times 10^{-3} \text{ mm}^3$ to $6.75 \times 10^{-3} \text{ mm}^3$) SS316L. The volume-loss is complemented by surface topography of worn surface in Fig. 6. The surface morphology reveals typical abrasive wear grooves, which were shallower in the laser-treated specimens (Fig. 6b) compared to untreated SS316L (Fig. 6a) that could result in lower volume-loss from laser surface treated SS316L specimens. Untreated stainless steels showed chipping (Fig. 6a) and cold-welding of wear debris to the parent surface that increased the roughness of surface and could have enhanced frictional forces to aggravate wear-loss. Cold-welding of wear particles in stainless steel is possible due to its high deformability; cold-welded particles get strain hardened and then fragmented due to brittle cracking with further straining during wear, as shown in Fig. 7. Marked increase in the volume-loss with increase in sliding distance from 300 m (8000 revolutions) to 900 m (24000 revolutions) was observed for both untreated and laser-treated SS316L. Greater wear-loss was observed for the specimen (both untreated and laser-treated SS316L) that slid for 900 m while the lowest was observed for the one that slid for 300 m distance.

Fig. 8 showed wear-rate after sliding to various distances from 300 to 900 m. Contrary to volume-loss results, wear-rate decreased with increase in sliding distance for both untreated and laser-treated stainless steel, though the wear-rates for both were very low ($<0.022 \times 10^{-3} \text{ mm}^3/\text{m}$). The highest wear-rate was experienced by specimen slid for 300 m, whereas, the lowest wear-rate was showed by those worn for 900 m distance for both untreated and laser-treated SS316L. This could be due the fact that the stainless steel shows strain hardening behavior associated with plastic deformation; increasing sliding distance could cause the hardening of the SS316L and, therefore, offer more resistance to wear-corrosion. It has also been shown earlier that the wear at different velocities (at 0.2 m/s and 1 m/s), resulted in different degree of deformation and could increase the micro-hardness of SS304L from $\sim 200 \text{ HV}$ to $>350 \text{ HV}$ [39]. It, however, decreased

with increase in distance from the worn surface (on the sub-surfaces) [39]. The mechanical wear rate (W) is related to hardness by a simple relationship (given below), though wear-rate also depends on other mechanical properties and corrosion [40]

$$W = K \cdot \frac{F}{H} \quad (1)$$

where F is frictional force, K is co-efficient of friction, and H is hardness of materials. Figs 5 and 8 showed better wear resistance for laser-treated stainless steel than untreated one for all distances. Higher hardness (H) of laser-treated specimens compared to untreated SS316L is one parameter that can contribute to the better wear resistance of laser-treated. Additionally, hardness is increased due to strain hardening and, in turn, it further improved the wear resistance of both laser-treated and untreated SS316L.

Since Ringer's solution (a representative of body fluid) is considered to be a corrosive medium as it contains high chloride concentration, the total volume-loss and wear-rate are expected due to corrosion in addition to mechanical wear. The anodic polarization (Fig. 4) for both laser-treated and untreated SS316L during wear is in the least corrosion (passive) state and, therefore, the contribution from corrosion would be very low. It is clear from earlier studies that the weight-loss from the wear test of steel under active and transpassive potential was much higher (by about 3 times) than that when it was under passive potential [41]. It can be seen from anodic polarization curves (Fig. 4) that the passive film resistance is increased after laser surface treatment (as passive current density reduced from $8 \mu\text{A}/\text{cm}^2$ for untreated SS316L to $<2.8 \mu\text{A}/\text{cm}^2$ for laser surface treated SS316L) and, thus, contribution to weight-loss due to corrosion during wear-corrosion is expected to be lower compared to untreated SS316L. The passive film may further reduce the frictional force (increases lubrication) and so reduced the wear. Galvanic corrosion between two counter surfaces (such as pin and disc) is known to contribute weight-loss to a great extent during sliding wear in corrosive environment [42]. Coupling between ceramics and stainless steel, such as in the present study, do not favor this form of corrosion while in sliding, ceramic being a non-conducting. Thus, this mode of corrosion (galvanic) is likely to cause insignificant weight-loss of pin and stainless steel disc, as noticed in the present study. Pitting, however, is probable if surface roughness enhances (such as due to wear) that favors the formation of extremely acidic solution with high chloride concentration (in sites such as wear grooves). This could cause the pitting in addition to general corrosion on the worn surface of untreated SS316L and laser-treated at $<1200 \text{ W}$ (Table III) as shown Fig. 9a and b. Pitting, though, does not directly cause significant increase in the weight-loss (in corrosion studies), increasing pit density on the surface can assist wear by reducing the strength of the counter surfaces and result in higher weight-loss.

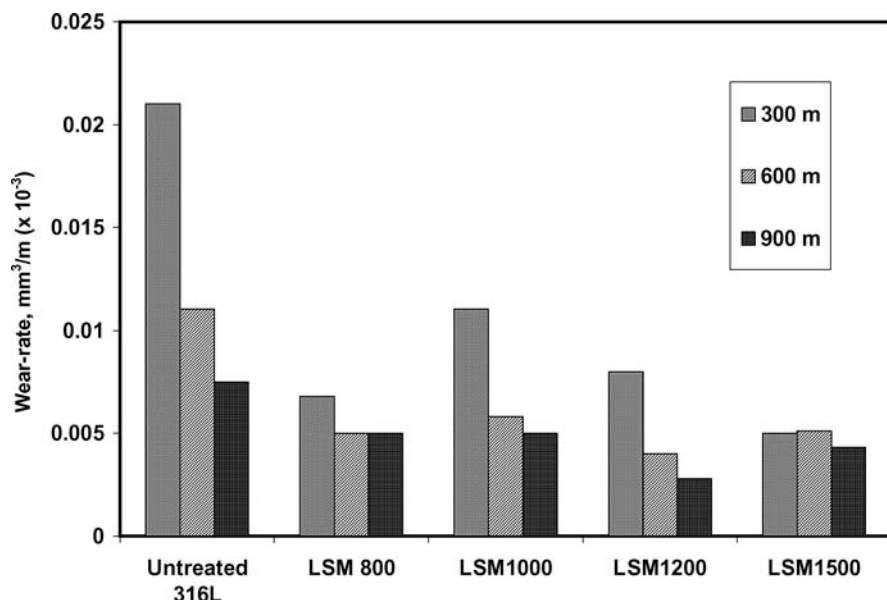


Figure 8 Wear-rate of untreated and laser-treated SS316L.

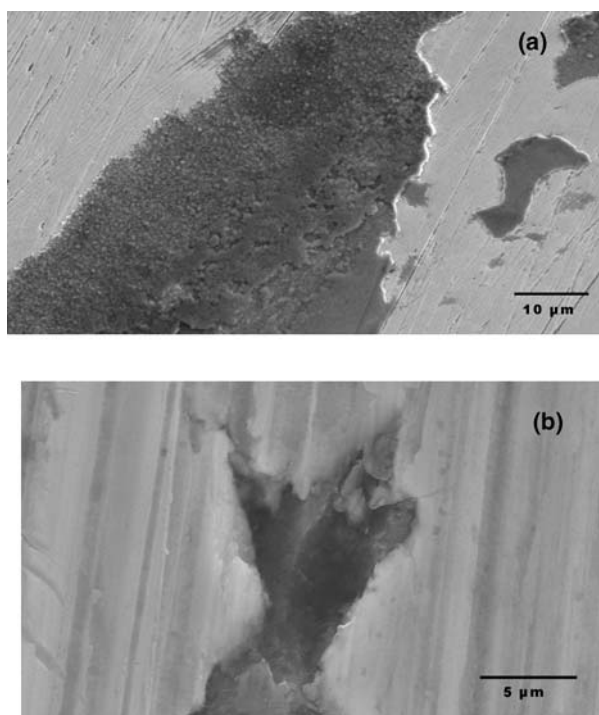


Figure 9 (a) General and (b) pitting corrosion in the wear track of untreated SS316L.

4. Summary

The microstructure and XRD pattern of untreated and of laser-treated SS316L showed austenitic phase, latter indicated possibility of crystallographic orientation along γ (200) plane at higher laser power (>800 W).

Laser treatment produced microstructure that contained refined (as low as $\sim 4 \mu\text{m}$) columnar regions. Micro-hardness of the laser-modified microstructure was higher (143–171 HV depends on the orientation of columnar grains) than the untreated SS316L (131 HV).

The passivation of SS316L was improved after laser-processing. The passivation current density for untreated SS316L was $\sim 8 \mu\text{A}/\text{cm}^2$ that reduced to below $2.8 \mu\text{A}/\text{cm}^2$ after laser surface treatment. The

pitting corrosion resistance of laser-treated at >1000 was higher (pitting potential $>+344$ mV) than the untreated SS316L ($\sim+310$ mV).

The volume-loss during wear and wear-rate were significantly low for laser-processed SS316L ($<4.54 \times 10^{-3} \text{ mm}^3$) than for untreated specimen ($>6.26 \times 10^{-3} \text{ mm}^3$). Abrasive wear was main wear mechanism, though brittle cracking and pitting were also observed in the worn surface of untreated stainless steel.

The study suggests that the laser surface treatment (>1000 W laser power) is a viable method to improve corrosion and tribological properties of SS316L for biomedical applications. This may significantly reduce the release of metal ions and wear-debris in the body and enhance the biocompatibility of implant devices made from SS316L.

Acknowledgement

One of the authors (Raghuvir Singh) sincerely acknowledges the financial assistance provided by the Department of Science & Technology, Government of India, for his visit to the University of Tennessee under BOYSCAST fellowship program.

Reference

1. F. ESCALAS, J. GALANTE, W. ROSTOKER and P. S. COOGAN, *J. Biomed. Mater. Res.* **9** (1975) 303.
2. M. SHIVA KUMAR, U. KAMACHI MUDALI and S. RAJESWARI, *J. Mater. Sci. Lett.* **13** (1994) 142.
3. U. I. THOMANN and P. J. UGGOWITZER, *Wear* **239** (2000) 48.
4. J. A. DISEGI and L. ESCHBACH, *Injury* **31** (2000) S-D2.
5. T. M. SRIDHAR, U. K. MUDALI and M. SUBBAIYAN, *Corros. Sci.* **45** (2003) 237.
6. R. SINGH and N. B. DAHOTRE, *J. Biomedical Materials Research: Part B—Applied Biomaterials* (2005) (submitted for publication).
7. S. MORAIS, J. P. SOUSA, M. H. FERNANDES, G. S. CARVALHO, J. D. BRUIJN and C. A. BLITTERSWIJK, *Biomaterials* **19** (1998) 999.
8. C. C. SHIH, C. M. SHIH, Y. Y. SU, L. H. SUI, M. S. CHANG and S. J. LIN, *Corros. Sci.* **46** (2004) 427.

9. M. SUMITAA, T. HANAWAB and S. H. TEOH, *Mater. Sci. Eng. C* **24** (2004) 753.
10. D. C. MEARS, *Intl. Metals Rev.* **22** (1977) 119.
11. N. HALLAB, J. J. JACOBS and B. JONATHAN, *Biomaterials* **21** (2000) 1301.
12. C. LIDEN, J. E. WAHLBERG and H. I. MARIACHI, in "Metal Toxicology," edited by R. A. Gayer (Academic Press, New York 1995), p. 447.
13. C. R. ANGLE, in "Metal Toxicology," edited by R. A. Gayer, C. D. Klaassen and M. P. Waalkes (Academic Press, New York, 1995), p. 71.
14. P. A. LABOR, A. B. REVELL, S. GRAY, G. T. WRIGHT and M. A. R. RAILTON, *J. Bone Jt. Surg.* **73** (1991) B:25.
15. A. W. PARKER, J. D. DREZ and J. T. JACOBS, *Am. J. Knee Surg.* **6** (1993) 129.
16. T. R. ANTHONY and H. E. CLINE, *J. Appl. Phys.* **49** (1978) 3203.
17. E. MCCAFFERTY and P. G. MOORE, *J. Electrochem. Soc.* **133** (1986) 1090.
18. N. PARVATHAVARTHINI, R. K. DAYAL, R. SIVAKUMAR, U. K. MUDALI, R. K. DAYAL, J. B. GNANAMOORTHY, S. M. KANETKAR and S. B. OGALE, *Trans. JIM* **32** (1991) 845.
19. R. A. SILVA, M. A. BARBOSA, R. VILLAR, O. CONDE, M. D. CUNHA BELO and I. SUTHERLAND, *Clin. Mater.* **7** (1991) 1.
20. J. STEWART and D. W. WILLIAMS, *Corros. Sci.* **33** (1997) 457.
21. U. KAMACHI MUDALI and A. BHARATI, *Mater. Sci. Tech.* **8** (1992) 1070.
22. U. K. MUDALI and R. K. DAYAL, *Mater. Eng. Perform.* **1** (1992) 341.
23. O. V. AKGUM, M. URGEN and A. F. CAKIR, *Mater. Sci. Eng.* **A203** (1995) 324.
24. Q. Y. PAN, W. D. HUANG, R. G. SONG, Y. H. ZHUO and G. L. ZHANG, *Surf. Coat. Technol.* **102** (1998) 245.
25. C. T. KWOK, F. T. CHENG and H. C. MAN, *ibid.* **99** (1998) 295.
26. *Idem.*, *Mater. Sci. Eng.* **A290** (2000) 55.
27. T. M. YUE, J. K. YU and H. C. MAN, *Surf. Coat. Technol.* **137** (2001) 65.
28. C. C. SHIH, C. M. SHIH, Y. Y. SU, J. L. SU, M. S. CHANG and S. J. LIN, *Corros. Sci.* **46** (2004) 427.
29. P. H. CHONG, Z. LIU, X. Y. WANG and P. SKELDON, *Thin Solid Films* **453/454** (2004) 388.
30. R. SINGH, M. MARTIN and N. B. DAHOTRE, *Surf. Eng.* (2004) (Accepted for publication)
31. N. B. DAHOTRE, Ph.D. Dissertation on Laser (2 KW Continuous Wave CO₂ laser) Melting and Alloying of Steel with Chromium (Michigan State University, 1987), p. 83.
32. C. G. WAKADE, N. B. DAHOTRE and K. MUKHERJEE, *Mater. Sci. & Eng.* **64** (1984) 247.
33. R. SINGH, A. KURELLA and N. B. DAHOTRE, *J. Biomater. Appl.* (2005) (accepted for publication).
34. N. YOSHIKUNI and N. KAZUTOSHI, *ISIJ Intern.* **33** (1993) 934.
35. C. L. MCBEE and J. KRUGHER, *Electrochim. Acta* **17** (1972) 1377.
36. A. BARBUCCI, G. CERISOLA and P. L. CARBOT, *J. Electrochem. Soc.* **149** (2002) B534.
37. S. V. PHADNIS, A. K. SATPATI, K. P. MUTHE, J. C. VYAS and R. I. SUNDARESHAN, *Corros. Sci.* **45** (2003) 2467.
38. Y. S. LIM, J. S. KIM and H. S. KWON, *J. Nucl. Mater.* **336** (2005) 65.
39. G. STRAFFELINI, D. TRABUCCO and A. MOLINARI, *Metall. Trans.* **33A** (2002) 613.
40. E. HORNBOGEN, in "Metallurgical Aspects of Wear," edited by A. R. Nicoll (1981) p. 28.
41. E. BROSZEIT, in "Metallurgical Aspects of Wear," edited by A. R. Nicoll (1981) p. 183.
42. P. A. DEARNLE and G. ALDRICH-SMITH, *Wear* **256** (2004) 491.

*Received 10 February
and accepted 11 April 2005*